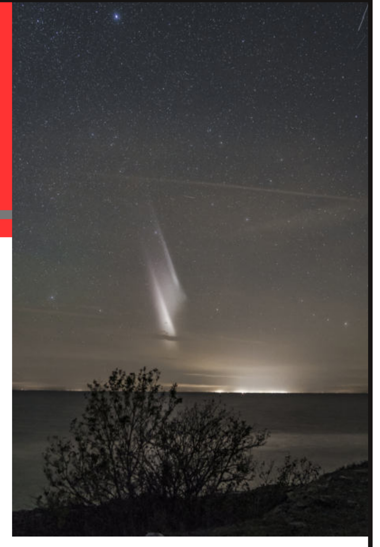

STEVE phenomenon related subauroral aurora or aurora-like luminous ionospheric structures – relevant structures, characteristics and correlations with geomagnetic storms derived from a citizen science based data package

Michael Hunnekuhl[1]*, Elizabeth MacDonald[2], Ben Swanson[3], Michael Theusner[4], James Stone[3], Alexei Chernenkoff[5], Stephen Voss[6], Jonathan Esling[3], Will Standring[7]

[1]Eichenweg 15, 30989 Gehrden, Germany, [2]NASA Goddard Space Flight Center, Greenbelt, MD, US, [3]Aurora Australis Tasmania Facebook group, [4]Am Knill 29a, 22147 Hamburg, Germany, [5]Alberta Aurora Chasers Facebook group, Alberta, Canada, [6]Administrator of the Aurora Australis Facebook group, New Zealand, [7]Tasmanian artist and photographer, Tasmania, Australia

**michael_hunnekuhl@web.de*

Abstract

STEVE (**S**trong **T**hermal **E**mission **V**elocity **E**nhancement) phenomenon related structures received much attention in recent years. MacDonald et al. (2018) reports on a link between these ionospheric structures and the Subauroral Ion Drift for the first time. Gallardo-Lacourt et al. (2018) presents a first statistical analysis based on 28 events. This work analyses the correlation between geomagnetic storms and amateur observations on basis of a STEVE event list derived from amateur observations. This list covers solar cycle 23 and 24 and contains 178+ observation days, 150 of them with time. We present the development of the event list with an additional poster in session 2. Very recently, Archer et al. (2019) published first results for the height extension of a STEVE arc and picket fence structures. This work presents results for the height of rays in a picket fence and their drift velocity observed in Australia on 7 November 2015. We found that ray- and patch-like substructures, only visible on short exposed photographs, form the overlying whitish STEVE arc and analysed the drift velocity. We also present a phenomenological based classification scheme for STEVE structures that allow non-professionals to classify observed structures thus simplifying the search for specific substructure types for combined ground based/in-situ analyzes of STEVE events. We further present multiple substructures, currently not mentioned in the literature, including, amongst others, rayed STEVE arcs, poleward bent picket fence rays, confined optical structures in the base region of picket fences as well as torch-like structures evolving from the whitish STEVE arc.

Key Points

- **STEVE observation case study: height and drift velocity calculation for picket fence, drift velocity calculation for whitish STEVE arc, identification of picket fence rays bent to pole side and fine structured whitish STEVE arcs**
- **Description of STEVE substructures**
- **Classification scheme for STEVE substructures**
- **STEVE phenomenon related structures occur at any geomagnetic storm intensity category**

Picket fence height calculation - case study

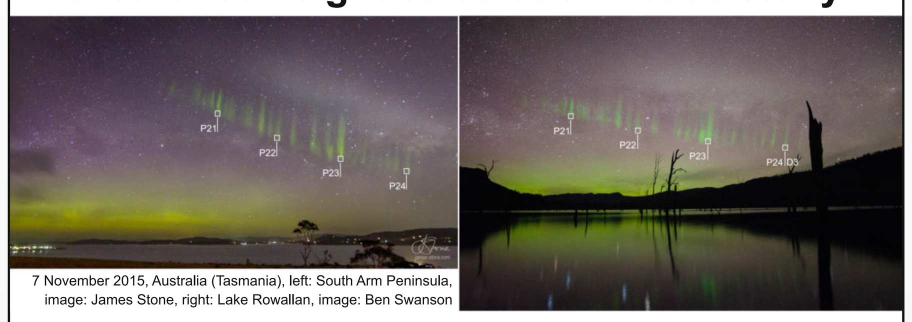

7 November 2015, Australia (Tasmania), left: South Arm Peninsula, image: James Stone, right: Lake Rowallan, image: Ben Swanson

- Problem: Accurate triangulation requires simultaneous images.
- Citizen science images of STEVE are not taken with deliberate simultaneity but can include master time series from one observer. Best fit of other images to master series
- Case study: 4 Tasmanian observers with same visible features as close as ~10 s seconds apart
- Solution: Tracking picket fence features and motion allows delay-tolerant high quality solutions appropriate for citizen scientist images from independent observers (assuming at least one has a time series)
- Method: Spherical trigonometry and Vicenty algorithm (Vincenty, 1975) for direct solutions for geodesics.
- Height for picket fence base: 19 heights, mean values ranging from **105.1 to 117.9 km**

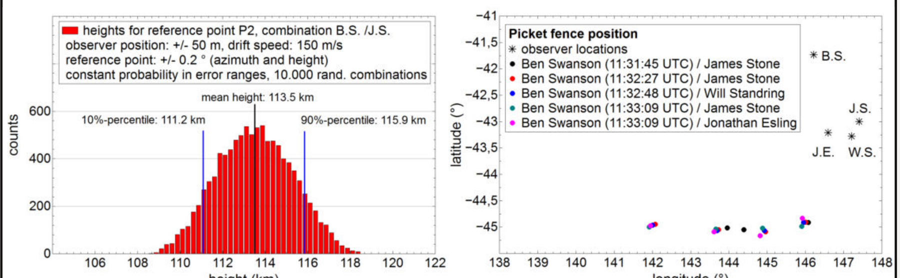

- Heights and positions calculated in 10.000 runs per reference point with observer positions and reference point view angles within the error ranges. Implementation of drift velocity allows to combine not-ideally time-matching images
- Error analysis robustly propagates uncertainties in observer locations and timing inaccuracy to resulting heights
- Consistent with results presented by Archer et al. (2019) but more robust method to account for non-simultaneous images

Drift speed calculations - case study

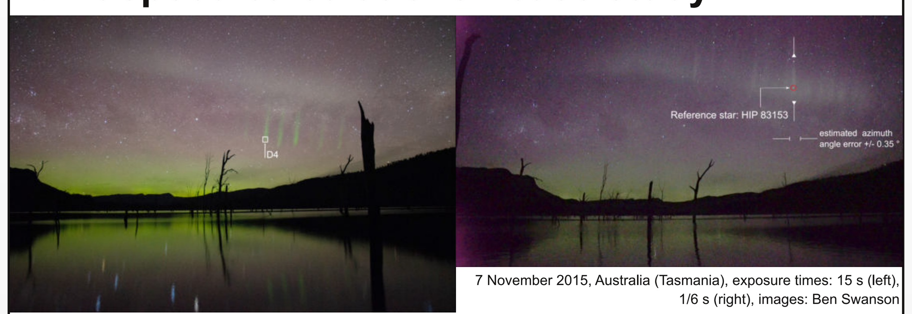

7 November 2015, Australia (Tasmania), exposure times: 15 s (left), 1/6 s (right), images: Ben Swanson

- Time for picket fence (left): 11:32-11:35 UTC, time for whitish STEVE arc (right): 11:40 UTC
- Real time video of the whitish part of STEVE arc observed on 7 November 2015 show ray- and patch-like structures drifting significantly faster westward than picket fence structures
- Video starts at ~11:34 UTC and shows picket fence and fast moving structures in parallel in the beginning
- Method for picket fence: Calculate drift velocity based on known altitude, position and azimuth drift over ~ 2 min and 7 images for two picket fence rays
- Method for STEVE arc: Identify trackable ray structure. Measure azimuth drift. Use picket fence position and orientation to convert azimuth drift motion to approximated drift velocity
- First approximation: white STEVE arc above foot points of picket fence base
- Second approximation: rays in whitish STEVE arc on same geomagnetic field lines as underlying picket fence structure. Drift speed with second approximation is ~ 10 % slower

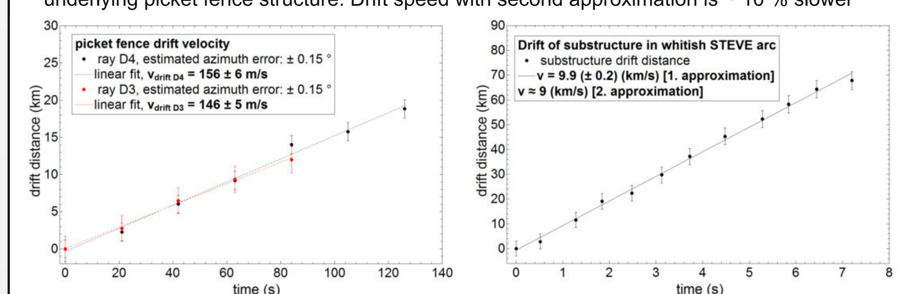

- Fine scale fast moving structures in STEVE arc observed in ~ 6 other events, analysis ongoing
- Need for shorter citizen science images to track structures and establish their characteristics

Geomagnetic storm related analysis

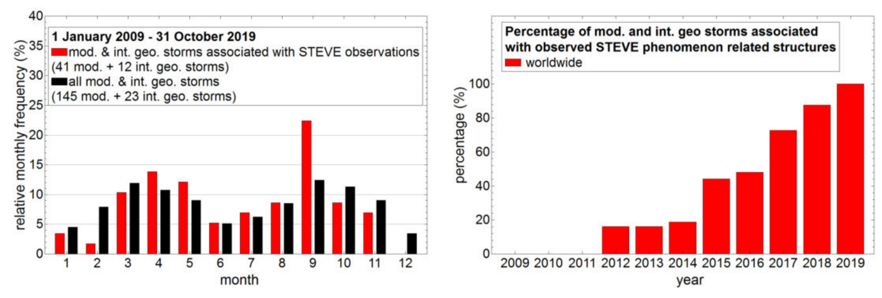

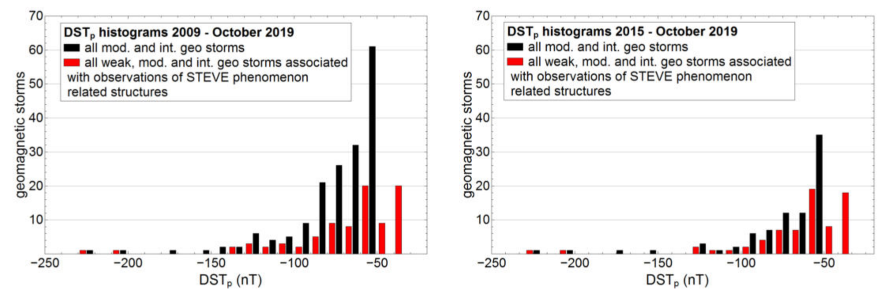

category	North America initial	main	recovery	sum	Southern Hemisphere initial	main	recovery	sum
weak	1	16	9	**26**	0	2	7	**9**
moderate	2	17	18	**37**	0	16	12	**28**
intense	0	4	2	**6**	1	7	5	**13**
sum	**3**	**37**	**29**	**69**	**1**	**25**	**24**	**50**
unknown time				**26**				**5**
quiet				**18**				**5**

Observation days (1 January 1996 - 31 October 2019)

category	Europe initial	main	recovery	sum	Worldwide initial	main	recovery	sum
weak	0	2	1	**3**	1	18	13	**32**
moderate	0	9	3	**12**	2	36	30	**68**
intense	0	2	0	**2**	1	10	7	**18**
sum	**0**	**13**	**4**	**17**	**4**	**64**	**50**	**118**
unknown time				**1**				**28**
quiet				**2**				**25**

Classification scheme & STEVE substructures

	Subauroral patches: Detached subauroral patches		Subauroral arcs: SAR-arcs		Detached subauroral arcs		STEVE phenomenon related structures: Picket fence		STEVE arcs & rays	
	code	feature	code	feature	code	feature	code	feature	code	feature
Color class	gg	green*	gg	green	gg	green*	gg	green*	gg	green
	rr	red	rr	red*	*rr*	*red*			pp	purple*
	uv	*ultraviolet*			*uv*	*ultraviolet*			*rr*	*red*
									ww	whitish*
Dynamic class	co	co-rotating	dp	poleward drift	ca	converging arc fragments	*de*	*drift eastward*	*de*	*drift eastward*
	de	*drift eastward*	dq	equatorward drift	cr	co-rotating	*dp*	*drift poleward*	*dp*	*drift poleward*
	dp	*drift poleward*			*de*	*drift eastward*	dq	drift equatorward	dq	drift equatorward
	dq	*drift equatorward*			*dp*	*drift poleward*	dw	drift westward	dw	drift westward
	dw	*drift westward*			*dq*	*drift equatorward*	tm	turbulent motion	fs	fast streaming
	pu	pulsating			*dw*	*drift westward*	wm	wave motion	pu	pulsating
					pu	pulsating			wm	wave motion
Substructure class	mp	multiple patches	ha	homogeneous (hom.) arc	ex	hom. arc with equartorward oriented extension(s)/undulations	bd	rays or patches bended poleward at base	ac	altitude separated color classes
	sp	single patch	he	hom. arc with embedded emission features	fa	fragmented arc	co	complex/turbulent ray or patch structures	*bd*	*rays or patches bended poleward at base*
			hx	hom. arc with north (N) or south (S) oriented extension(s)	ha	hom. arc	lf	latitudinal (lat.) separated picket fence	et	embedded torch
			mn	multiple hom. N-S separated arcs			lp	longitudinal (long.) quasi-periodically (qp.) arranged patches	fa	fragmented arc
			mx	multiple hom.arcs with N or S oriented extension(s)			lr	long. qp. arranged rays	fb	folded band(s)
							ma	multiple altitude separated structures	fp	fragmented arc with embedded patches
							rp	long. qp. arranged rays and/or patches	fr	fragmented arc with embedded rays
									gc	graded color class transition
									ha	hom. arc
									hp	hom. arc with embedded patches
									hr	hom. arc with embedded rays
									it	isolated torch
									la	lat. separated arcs or arc fragments
									mt	multiple embedded torches
									ry	rayed

(1) *: dominating color class in photographs, red: presence of feature is unclear (not analysed), (2) further specific features possible, (3) *ultraviolet*: mentioned by Moshupi et al. (1979) and Størmer (1942), not verified with COTS (commercial of-the-shelf) digital cameras by amateur photographers, verification test possible with full-spectrum-modified COTS digital cameras, (4) summary of non-STEVE subauroral aurora types presented by e.g. Frey (2007)

28 May 2017, USA, (Wyoming), torch-like STEVE structure, image: Jan Curtis

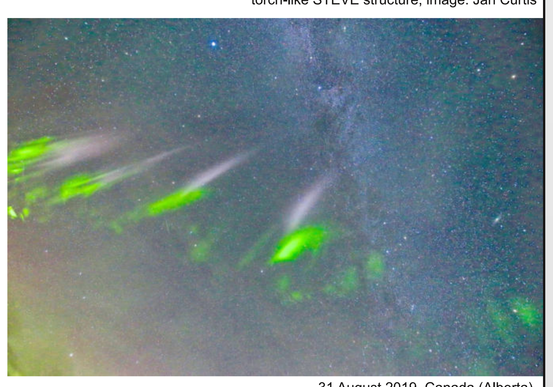

31 August 2019, Canada (Alberta), complex ray or patch picket fence structure, image: John Andersen

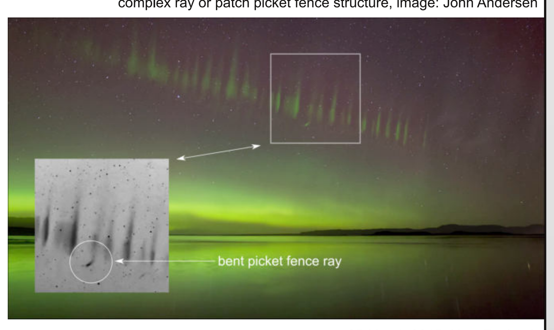

27 March 2017, New Zealand, poleward bent picket fence base, image:Stephen Voss

7 November 2015, 11:43 UTC, Australia (Tasmania), exposure time: 0.6 s, image: Ben Swanson

Rayed STEVE arcs: Literature describes STEVE arcs as east-west oriented well-defined arcs, sometimes spanning the sky from horizon to horizon, with a color composition dominated by a purple hue. All STEVE literature that includes STEVE arc photos present multiple second exposed photos. We found fine structured rays in STEVE arcs in multiple cases, e.g.: 2 June 2001, 2 August 2002, 7 September 2015, 20 September 2015, 7 November 2015, 10 April 2018 and 31 August 2019.

Bent picket fence: Rays in the common aurora are oriented, along local magnetic field lines. The base of picket fence rays is sometimes bent poleward. We found photographs showing bent picket fence rays in multiple cases, e.g.: 7 November 2015, 27 March 2017, 28 May 2017 and 16 September 2017.

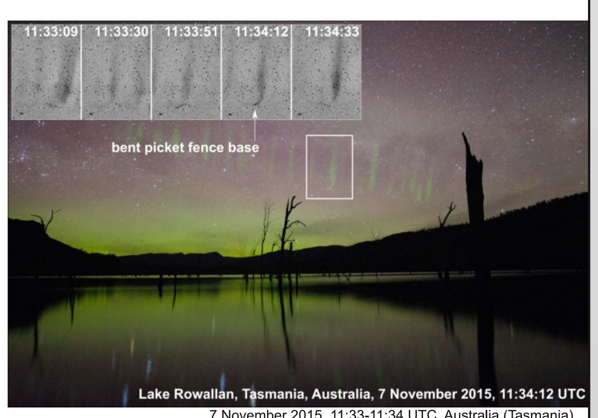

7 November 2015, 11:33-11:34 UTC, Australia (Tasmania), exposure time: 15 s, image: Ben Swanson

7 November 2015, 11:52 UTC, Australia (Tasmania), exposure time: 5 s, image: James Stone

Torch-like structures: Isolated ray- or pillar-like structures are well-known in the common aurora. We found STEVE arcs with torch-like structures, evolving from the whitish part of a STEVE arc. On unsaturated photographs, the color of these structures is dominated by a whitish color over their whole height extend above the picket fence altitude regime which is atypical for common auroral rays. We found isolated and arc-embedded torch-like STEVE structures in multiple cases, e.g.: 15 August 2015, 7 November 2015, 27 May 2017 and 31 August 2019.

7 November 2015, 11:41 (left), 11:52 (right) UTC, Australia (Tasmania), exposure times: 13 s (left), 15 s (right), images: Will Standring

More details on second poster in session 2

Picket fence - confined structures

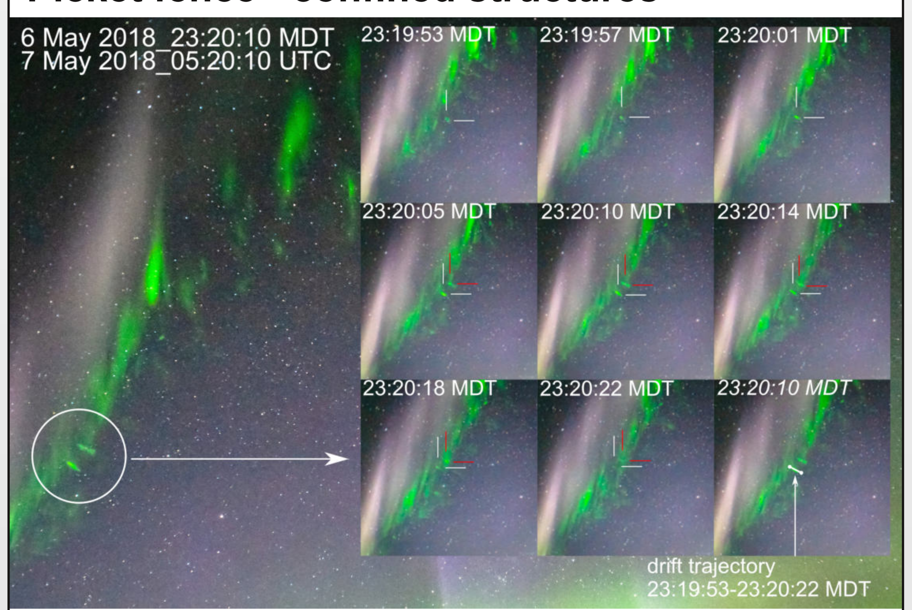

7 May 2018, Canada (Alberta), 05:20 UTC, exposure time: 4 s, images: Alexei Chernenkoff

We found evidence for confined optical structures in picket fences (4 events) characterized by a separation from the picket fence rays, in rare cases with orientations strongly deviating from the undisturbed Earth magnetic field orientation, analysis ongoing

References

Archer W. E. et al. (2019). The vertical distribution of the optical emission of a STEVE and picket fence event, Geophysical Research Letters, 46 (19), 10719–10725

Frey H. U. (2007). Localized Aurora Beyond the Aurora Oval, Reviews of Geophysics, 45, RG1003.

Gallardo-Lacourt B. et al. (2018). A Statistical Analysis of STEVE, JGR Space Physics, 123 (11), 9893–9905.

Hunnekuhl M. (2019). STEVE phenomenon related structures - detailed event list version 1.0, https://doi.org/10.17605/OSF.IO/HBGYA

MacDonald E. A. et al. (2018). New science in plain sight: Citizen scientists leads to the discovery of optical structure in upper atmosphere, Science Advances, 4 (3), eaaq0030.

Moshupi M. C. et al. (1979). Characteristics of through region auroral patches and detached arcs observed by ISIS 2, Journal of Geophysical Research, 84 (A4), 1333–1346.

Størmer C. (1942). Remarkable Aurora-Forms from Southern Norway. III – IX, Geofysiske Publiskasjoner, 13(7).

Vincenty T. (1975). Direct and inverse solutions of geodesics on the ellipsoid with application of the nested equations, Survey Review, 22, 88–93.]

Summary

- Analysis of correlations between STEVE phenomenon related structures and geomagnetic storms
- Case study: Calculation of picket fence altitude and drift velocity
- Definition of a phenomenological classification scheme for STEVE phenomenon related substructures extended to other subauroral auroral structures
- Identification of multiple new STEVE phenomenon related substructures

Outlook

- Implementation of characteristic structures in STEVE event list
- Altitude calculations for more events and specific structures
- Measurement of STEVE arc width
- Refinement of phenomenological classification scheme

Acknowledgments

We thank John Andersen, Jan Curtis and Jörgen Tannerstedt (photo in header) for permissions to use their images. This work is part of a non-funded volunteer project. E.M is supported by a NASA CAN award to the NASA Space Science Education Consortium.